Vanillin derivative as performing type I photoinitiator

Louise Breloy, Claire Negrell, Anne-Sophie Mora, Wing-Sze Jennifer Li, Vlasta Brezová, Sylvain Caillol, Davy-Louis Versace

Vanillin Derivative as Performing Type I Photoinitiator

L. Breloy[†], C. Negrell[§], A.-S. Mora[§], W. S. J. Li[§], V. Brezová[±], S. Caillol[§], D.-L. Versace*[†]

[†] Institut de Chimie et de Matériaux Paris-Est (ICMPE), Equipe Systèmes Polymères Complexes, CNRS-UPEC UMR 7182, 2-8 rue Henri Dunant-94320 Thiais, France

*Corresponding author: **versace@icmpe.cnrs.fr**

[§] ICGM, Univ Montpellier, CNRS, ENSCM, Montpellier, France.

[±] Slovak University of Technology in Bratislava, Faculty of Chemical and Food Technology, Institute of Physical Chemistry and Chemical Physics, Department of Physical Chemistry, Radlinského 9, SK-812 37 Bratislava, Slovak Republic.

ABSTRACT. A new efficient type I photoinitiator derived from vanillin was synthesized to initiate, according to a green photoinduced process, the free-radical polymerization (FRP) of acrylate monomers in a reduced time and under air. Interestingly, this unprecedented photoinitiator lead to high acrylate conversions even under air, with a higher efficiency than some reference photoinitiating systems commonly used in FRP.

Keywords: vanillin, natural oil acrylate monomer, free-radical polymerization, UV-light.

INTRODUCTION

Over the past twenty years, free-radical photopolymerization (FRP) has gained considerable interests for the synthesis of new smart and multifunctional materials with multiple conventional applications [1, 2] in microelectronics, coatings, adhesives, inks, dental fillings or the fabrication of 3D microstructures. The growing interest of FRP by industry and the increasing number of publications on the subject demonstrate that photopolymerization is becoming unavoidable. Many striking advantages of FRP can be pointed out over the thermal polymerization [3] such as low temperature process at room temperature or below, fewer side reactions, reactions proceed in a few seconds or minutes without any solvent, thus avoiding volatile organic compounds to be released; this makes FRP an environmentally-friendly technique. Up to date, FRP has been extensively described and numerous interesting reviews [1, 2] have been published. In this technology, polymerization occurs with the use of two types of photoinitiators [4-6] which differ in the way radical species are generated. Type I photoinitiators are aromatic carbonyl organic compounds [5] (benzil ketals, benzoin and derivatives, acetophenones, aminoalkyl phenones, O-acyl-α-oximino ketones, acylphosphine oxides, acylgermanes and α-hydroxyalkyl ketones) and undergo upon light absorption an "α-cleavage" to produce free-radical species. Interestingly, the photochemically generated phosphinoyl radicals are widely exploited due to their high reactivity arising from the high electron density around the phosphorus atom and favorable steric conditions [7, 8]. On the contrary, type II photoinitiating systems are capable of undergoing intermolecular H-abstraction or electron/proton transfer reactions when combined with co-initiators [9-13] (i.e. H-donors like tertiary amines, alcohols, ethers, silanes, germanes, stannanes or thiols) or with the use of α-ketoesters [14]. Benzophenone, thioxanthone, benzil, and quinone derivatives are typical bimolecular type II photoinitiators which lead in presence of H-donors to the formation of both ketyl radical and another radical derived from the H-donor molecule [15, 16]. However, it is assumed that the initiation of the polymerization according to a bimolecular type II reaction is slower than that of a type I process, suffer from back electron transfer and the resulting ketyl radicals are usually unreactive toward vinyl monomers due to their high stability and steric hindrance [17].

Another point raising is that the majority of the photoinitiators commonly used and described in literature are derived from petro-sourced molecules. Therefore, we focused our attention on the synthesis of a novel type I photoinitiator from a bio-sourced synthon. To the best of our knowledge, the synthesis and the photoreactivity of type I photoinitiators derived from

biosourced molecules have never been described yet. Thus, the development of a type I photoinitiator from natural synthons remains a challenge to face. If oils and polysaccharides are already well exploited at industrial scale, there is a lag concerning aromatic compounds. Among these aromatic derivatives, vanillin can be considered as the most promising compound in this research area. Indeed, this molecule is among the only few phenolic compounds which can currently be produced industrially from lignin [18]. Its interest comes not only from its availability: this molecule bears two reactive groups strategic for organic modifications, a phenol and an aldehyde, and offers the great advantage to be safe. Main applications of vanillin nowadays concern perfumery of food industry, but vanillin derivatives have also a great potential as antibacterial agents [19], for drug delivery [20], flame retardation [21, 22], composites [23]. It was highlighted as a very promising building block for the preparation of bio-based monomers [24] and renewable polymers, more particularly high-performance thermosets [25].

Here, we report for the first time, the synthesis of a new vanillin-derived type I photoinitiator and evaluate its capability to initiate in laminate and under air the FRP of two acrylate monomers: trimethylolpropane triacrylate (TMPTA), which is a reference monomer for FRP studies, and Soybean oil epoxidized acrylate (SOA), a cheap and natural oil acrylate monomer. Its properties have been compared with those of classical type I and type II photoinitiating systems. The addition of a thiol cross-linker, trimethylolpropane *tris*(3-mercaptopropionate) (TT) was experimented to reduce oxygen sensitivity of the new vanillin-derived photoinitiator. Mechanisms of photopolymerization process were described by electron paramagnetic resonance (EPR) and laser-flash Photolysis (LFP), and kinetic studies were carried out by real-time Fourier transform infrared spectroscopy (RT-FTIR).

EXPERIMENTAL SECTION

Materials. 2,2-Dimethoxy-2-phenylacetophenone (DMPA), phenyl*bis* (2,4,6-trimethylbenzoyl)-phosphine oxide (BAPO) and trimethylolpropane triacrylate (TMPTA) were kindly provided by BASF and Sartomer, respectively. Soybean oil epoxidized acrylate (SOA), trimethylolpropane *tris*(3-mercaptopropionate) (TT, ≥ 95%), 1-hydroxy-cyclohexyl-phenyl-ketone (HCPK, 99%), Quinizarin (QUI, 96%), Purpurin (PUR, dye content 90%), allyl bromide, potassium carbonate (K_2CO_3), diphenylphosphine oxide, activated manganese oxide (MnO_2) and celite were all provided by Sigma-Aldrich. 9,10-Anthraquinone (AQ, > 98%) and thioxanthone (TX, > 98%) were provided by Alfa Aesar and TCI respectively. Vanillin was also

purchased from Alfa Aesar and used without any treatment. Table 1 describes the chemical structure of the main compounds used in this study.

Table 1. Structure of the compounds used in this study.

Name	Structure	Used as
Vanillin	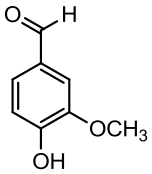	Scaffold for the synthesis of type I photoinitiator
Quinizarin (QZ)	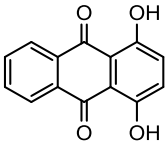	Photosensitizer
Purpurin (PUR)	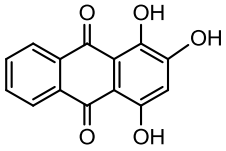	Photosensitizer
2,2-Dimethoxy-2-phenylacetophenone (DMPA)	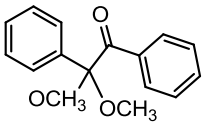	Type I photoinitiator
1-Hydroxy-cyclohexyl-phenyl-ketone (HCPK)	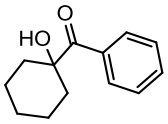	Type I photoinitiator
Phenyl*bis* (2,4,6-trimethylbenzoyl)-phosphine oxide (BAPO)	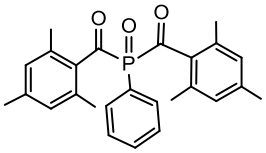	Type I photoinitiator
Trimethylolpropane *tris*(3-mercaptopropionate) (Trithiol, TT)	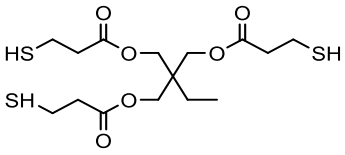	Thiol monomer /reticulating agent

Trimethylolpropane triacrylate (TMPTA)	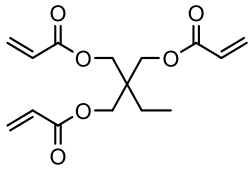	Triacrylate monomer
Soybean oil epoxidized acrylate (SOA)	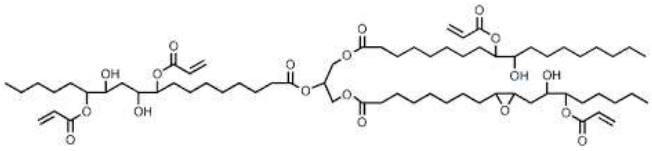	Bio-sourced Acrylate monomer

Methods. Proton, carbon and phosphorus Nuclear Magnetic Resonance (^{1}H, ^{13}C, ^{13}C – APT, ^{13}C – DEPT 135 and ^{31}P NMR) analyses were performed in deuterated chloroform ($CDCl_3$) using a Bruker Avance 400 MHz NMR spectrometer at a temperature of 25 °C. NMR samples were prepared as follows: 10 mg of product for ^{1}H and ^{31}P experiment and 50 mg of product for ^{13}C NMR, ^{13}C – APT and ^{13}C – DEPT 135 in around 0.4 mL of $CDCl_3$. The chemical shifts were reported in part per million relatives to tetramethylsilane. Spin multiplicity is shown by s = singlet, d = doublet, t = triplet, m = multiplet. MS measurements were performed on a Waters Synapt G2-S High Resolution Mass Spectrometer (HRMS) equipped with an ESI ionization source.

Synthesis of 4-allyloxy-3-methoxybenzaldehyde (A). Vanillin (1 eq, 20.0 g, 131 mmol) was combined with dimethylformamid (DMF) in a round-bottom flask in an ice bath. K_2CO_3 (4 eq, 72.7 g, 52.8 mmol) was added and left to stir for 3 min. Allyl bromide (4 eq, 63.6 g, 52.8 mmol) was added via syringe dropwise and stirred for 30 min. After, the reaction mixture was stirred for 48 h at 25 °C. 700 mL of deionized water was added to the reaction mixture and the aqueous phase was extracted with ethyl acetate (3 x 700 mL). Organic phase was washed with 700 mL of brine. Organic phase was dried with Na_2SO_4 and ethyl acetate was removed by rotary evaporator. Lastly, the product was purified by distillation under reduced pressure (10^{-2} mBar and 60 °C). Isolated yield = 59%. **^{1}H NMR** (ppm, 400.13 MHz, $CDCl_3$) δ: 3.96 (O-C**H**$_3$, 3H, s), 4.73 (O-C**H**$_2$-CH, 2H, d), 5.37 (CH=C**H**aHb, 1H, d, J_{cis}=10.5 Hz), 5.47 (CH=CHa**H**b, 1H, d, J_{trans}=17.3 Hz), 6.11 (CH_2-C**H**=CH_2, 1H, m), 7.00 ($H_{aromatic}$, 1H, d), 7.44 ($H_{aromatic}$, 1H, s), 7.45 ($H_{aromatic}$, 1H, d), 9.87 (**H**C=O, 1H, s). **^{13}C NMR** (ppm, 100.61 MHz, $CDCl_3$) δ: 56.1 (O-**C**H_3), 69.8 (O-**C**H_2-CH), 109.3 ($CH_{aromatic}$), 111.9 ($CH_{aromatic}$), 118.8 (CH=**C**H_2), 126.6 ($C_{Haromatic}$), 130.0 (HC(O)-**C**$H_{aromatic}$), 132.2 (**C**H=CH2), 149.8 (CH_3-O-**C**$H_{aromatic}$), 153.5 (CH_2-

O-**C**$H_{aromatic}$), 191.0 (H**C**=O). **HRMS** (m/z, ES+, [M+H+]): $C_{11}H_{13}O_3$; Calculated 193.0865; found 193.0867.

Synthesis of α-hydroxy(4-allyloxy-3-methoxybenzyl)diphenylphosphine oxide (B). 4-allyloxy-3-methoxybenzaldehyde (1 eq, 14.0 g, 72.8 mmol), diphenylphosphine oxide (1 eq, 14.7 g, 72.8 mmol), and dry tetrahydrofuran (THF; 280 mL) were combined in a round-bottom flask and sealed with a septum. Triethylamine (1 eq, 7.37 g, 72.8 mmol) was added dropwise into the reaction mixture at 25 °C and stirred for 24 h. The precipitated product was filtered and washed with THF several times and then dried. It used without further purification for next step. Isolated yield = 85%. **^{1}H NMR** (ppm, 400.13 MHz, $CDCl_3$) δ: 3.45 (O-C**H**$_3$, 3H, s), 4.51 (O-C**H**$_2$-CH, 2H, d), 5.25 (CH=C**Ha**Hb, 1H, d, J_{cis}=9.3 Hz), 5.34 (HO-C**H**, 1H, s), 5.38 (CH=CHa**Hb**, 1H, d, J_{trans}=17.2 Hz), 5.96 (O**H**, 1H, s), 6.06 (CH_2-C**H**=CH_2, 1H, m), 6.55 ($H_{aromatic}$, 1H, d), 6.61 ($H_{aromatic}$, 2H, s), 7.32 ($H_{aromatic}$ in meta position of P, 4H, m), 7.45 ($H_{aromatic}$ in para position of P, 2H, m), 7.68 ($H_{aromatic}$ in ortho position of P, 4H, m). **^{13}C NMR** (ppm, 100.61 MHz, $CDCl_3$) δ: 55.5 (O-**C**H_3), 69.7 (O-**C**H_2-CH), 73.1-74.0 (**C**H-OH), 110.9 (**C**$H_{aromatic}$), 112.5 (**C**$H_{aromatic}$), 117.9 (CH=**C**H_2), 120.2 (**C**$H_{aromatic}$), 128.1 (**C**$H_{aromatic}$ in meta position of P), 129.8 (HO-CH-**C**$H_{aromatic}$), 130.3 (P-**C**$H_{aromatic}$), 131.8 (**C**$H_{aromatic}$ in para position of P), 132.1-132.5 (**C**$H_{aromatic}$ in ortho position of P), 133.3 (**C**H=CH_2), 147.5 (CH_3-O-**C**$H_{aromatic}$), 148.7 (CH_2-O-**C**$H_{aromatic}$). **^{31}P NMR** (ppm, 161.98 MHz, $CDCl_3$) δ: 30.8. **HRMS** (m/z, ES+, [M+H+]): $C_{23}H_{24}O_4P$; Calculated 395.1412; found 395.1415.

Synthesis of (4-allyloxy-3-methoxybenzoyl)diphenylphosphine oxide (PM). A solution of α-hydroxy(4-allyloxy-3-methoxybenzyl)diphenylphosphine oxide (1 eq, 11.0 g, 2.79 mmol) in anhydrous dichloromethane (DCM; 220 mL) and activated MnO_2 (1 eq, 48.5 g, 558 mmol) in a round-bottom flask and purge for 30 min under N_2. The mixture was stirred to react at 25°C for 18 h. Then it was filtered under celite and DCM was removed by rotary evaporator. Isolated yield = 95%. **^{1}H NMR** (ppm, 400.13 MHz, $CDCl_3$) δ: 3.93 (O-C**H**$_3$, 3H, s), 4.72 (O-C**H**$_2$-CH, 2H, d), 5.35 (CH=C**Ha**Hb, 1H, d, J_{cis}=10.1 Hz), 5.43 (CH=CHa**Hb**, 1H, d, J_{trans}=17.1Hz), 6.08 (CH_2-C**H**=CH_2, 1H, m), 6.95 (**H**$_{aromatic}$, 1H, d), 7.5-7.9 (**H**$_{aromatic}$, 10H, m). **^{13}C NMR** (ppm, 100.61 MHz, $CDCl_3$) δ: 56.0 (O-**C**H_3), 69.8 (O-**C**H_2-CH), 111.0 (**C**$H_{aromatic}$), 112.7 (**C**$H_{aromatic}$), 118.4 (CH=**C**H_2), 118.9 (**C**$H_{aromatic}$), 128.8 (**C**$H_{aromatic}$ in meta position of P), 132.1-132.4 (**C**$H_{aromatic}$), 149.5 (CH_3-O-**C**$H_{aromatic}$), 154.3 (CH_2-O-**C**$H_{aromatic}$). Traces of MnO_2 in the sample of photoinitiator did not allow to obtain a correct ^{31}P NMR spectrum. **HRMS** (m/z, ES+, [M+H+]): $C_{23}H_{22}O_4P$; Calculated 393.1256; found 393.1261.

UV-Visible absorption spectra of the photoinitiators were measured using a Perkin Elmer Lambda 2 UV–vis spectrophotometer in the 200–800 nm wavelength range.

Photopolymerization kinetic studies. For each sample, photoinitiator (PI) and TT (PI/TT 1%/1% w/w with respect to the monomer) were dissolved in acrylate monomer (TMPTA or SOA). Formulations were stirred and sonicated for 15 min before study. The resulting photosensitive formulations were laid down on a BaF_2 pellet and irradiated with Hg-Xe lamp (Lightningcure LC8-02 lamp from Hamamatsu, 200 W, 60 $mW.cm^{-2}$) under air or in laminate. The thickness of the coatings was 12 μm for all experiments. The decrease of acrylate functions of TMPTA or SOA was continuously followed at 1636 cm^{-1} by real-time Fourier transform infrared spectroscopy (RT-FTIR, JASCO FTIR 4700) according to previously described method [26].

Laser-flash photolysis studies (LFP). LFP experiments were performed according to previously described procedures [27, 28] and employed the pulses from a Spectra Physics GCR-150-30 Nd:YAG laser (355 nm, 7 ns pulse length). Experimental conditions for each measurement are detailed in the results section. For recording the transient absorption spectra and quenching studies with oxygen or TT, solutions of PM were prepared with an absorbance value ~0.6 at the excitation wavelength (355 nm) in an UV-cell with a path length of 1 cm.

EPR experiments. The X-band EPR spectra were measured by means of EMX*plus* spectrometer (Bruker) at 100 kHz modulation frequency with a high sensitivity probe-head (Bruker) using thin-walled quartz EPR tubes (Bruker). As the spin trapping agents 5,5-dimethyl-1-pyrroline *N*-oxide (DMPO, Sigma-Aldrich, distilled before use) or *N*-tert-butyl-α-phenylnitrone (PBN, Sigma-Aldrich) were applied. The samples prepared by the mixing of stock solutions in benzene were carefully saturated with argon. The prepared solutions were irradiated at 293 K directly in the EPR resonator using a LED@385 nm source (λ_{max} = 385 nm; Bluepoint LED, Hönle UV Technology) and the EPR spectra were recorded *in situ* during exposure. The *g*-values of spin-adducts were determined with an uncertainty of ± 0.0001 using a nuclear magnetic resonance teslameter and integrated frequency counter. The experimental EPR spectra were analyzed by Bruker software WinEPR and the simulated spectra were calculated with the EasySpin toolbox as previously described [27, 28].

RESULTS and DISCUSSION

Both acyl-phosphine oxides are known to be used as classical photoinitiators. A methodology has been described by Nazir and co-workers [29]. First, the addition of aldehydes to diphenylphosphine oxide in dry solvent in the presence of base, gives α-hydroxyphosphine oxides, which are oxidized to desired acyl-phosphine oxides by MnO_2. We used this synthesis on a derivative of vanillin to obtain a partially bio-based photoinitiator. To avoid the negative influence of the phenolic group of vanillin, which could lead for example to side reactions such as the addition of phenol group in basic media to the aldehyde or could play as a radical scavenger during free-radical photopolymerization, an allylation with allyl bromide was done in mild conditions with a soft base K_2CO_3 at room temperature, according to a previously described procedure [24]. The product (A) was characterized by ^{1}H and ^{13}C NMR (Figures S1 and S2 in supporting information). The chemical shifts at 4.73, 5.37, 5.47 and 6.11 ppm were attributed to protons on O-CH_2 and double bond function (CH=CH_2) grafted on aromatic cycle, respectively, thus demonstrating the success of the allylation. The ^{13}C NMR spectrum confirmed this grafting by the appearance of allyl bond signals at 118 and 133 ppm. The synthesis of acyl-phosphine oxide was then achieved in two steps: first, the addition reaction between allyl vanillin and the phosphine (step 2) was performed and secondly the hydroxyl group in α position of phosphine oxide was oxidized into ketone. Figures S3 and S4 display respectively the ^{1}H and ^{13}C NMR spectra of the α-hydroxy(4-allyloxy-3-methoxybenzyl)diphenylphosphine oxide (B, Scheme 1) obtained after 24 hours at room temperature (25°C) and a step of purification by precipitation. Figure S3 clearly shows new chemical shifts around 7.3-7.7 ppm characteristic of aromatic protons of phosphine oxide, the appearance of the CH in α-position of hydroxyl function at 5.34 ppm and the disappearance of the aldehyde proton at 9.87 ppm. Moreover, the carbon labelled 1 and bearing the hydroxyl function (Figures S4 and S5) displays a chemical shift around 74 ppm. The ^{31}P NMR spectrum presented in Figure S6 demonstrated the phosphorylation of aldehyde function with diphenylphosphine oxide by the appearance of phosphine signal at 30.8 ppm. In step 3, the oxidation of the hydroxyl functions was mainly highlighted by the disappearance of the CH in α-position of hydroxyl function at 5.34 ppm shown in the ^{1}H NMR spectrum in Figure S7 and the disappearance of the ^{13}C signals at 74 and 73 ppm (see Figure S8 in comparison with Figure S5). This innovative photoinitiator was achieved with a global yield of 50%. As illustrated in Figure S9, the UV-vis absorption spectrum of PM shows a higher molar extinction coefficient than DMPA, HCPK or BAPO used as references for type I photoinitiator. The overlap of the

emission spectrum of the Hg-Xe lamp (Figure S10) with the UV-Vis absorption spectra of PM makes it a potential photoinitiator.

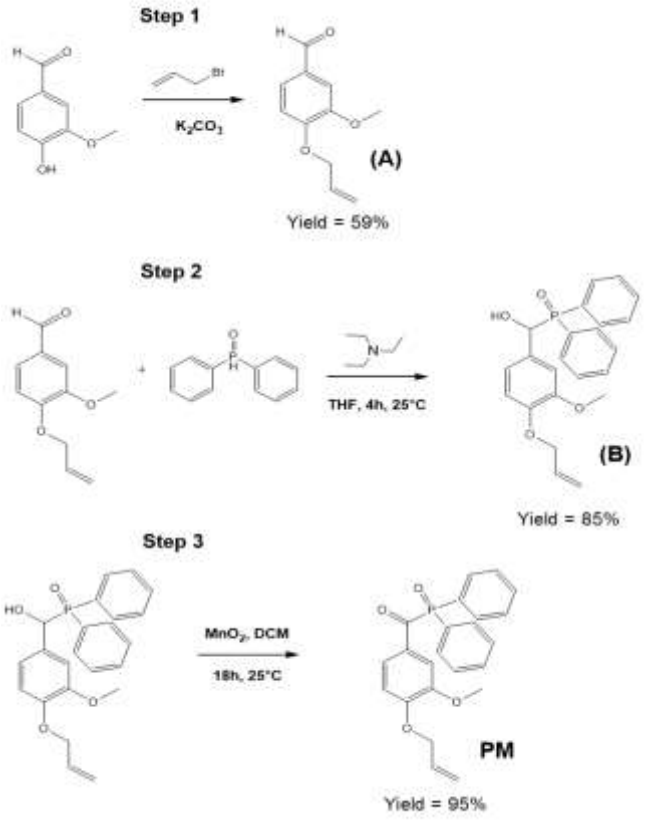

Scheme 1. General procedure for the synthesis of the new vanillin-derived type I photoinitiator.

Previous studies from Turro [30, 31] and Schnabel [7, 32] investigated the reactivity of phosphine oxides derivatives under UV-light irradiation ($\lambda_{excitation}$ = 355 nm) by LFP. They demonstrated that upon UV-light exposure, these photoinitiators underwent an homolytic photocleavage to produce benzoyl radicals and diphenylphosphinoyl radicals which are readily observable around 330 nm. No other active radical species were detected. To go further in the mechanism approach that we suggest during the photolysis of PM, EPR-ST technique is coupled with LFP experiments. EPR-ST is much more sensitive than LFP technique to observe short-lived and highly reactive free radicals in chemical systems at low concentration [33]; The generated spin-adducts possess considerably greater stability than that of the parent free radical species; for instance, phenyl radicals are not easily detected by LFP as λ_{max} = 240 nm [34], LFP equipment lacks sensitivity for absorptions less 300 nm [34] and the signal of some phenyl derived radicals can be merged with diphenylphosphinoyl radicals between 320 and 380 nm

[35]. Therefore, the generation of non-persistent radical species upon photoexcitation of PM was first monitored by EPR spin trapping technique. *In situ* irradiation of PM by LED@385 nm source in the presence of PBN spin trap results in the substantial intensity growth of complex EPR signal, corresponding to the simultaneous formation of •PBN-adducts of carbon- and phosphorus-centered radicals (Figure 1). Simulation was calculated considering the presence of four •PBN-adducts with the spin-Hamiltonian parameters summarized in Table 2. Scheme 2 describes the proposed homolytic cleavage of PM under light exposure. Interestingly, PM generates four radical species, i.e. two phosphorus and two carbon-centered radicals, which can be used as photoinitiating species for the FRP of acrylates (see Supporting Information). One forces to note that the signals of PBN spin-adducts of substituted benzoyl radical (Table 2) are less intensive than those of phosphinoyl radicals because of their lower rates of formation and faster rate of relaxation compared to that of phosphinoyl radicals according to Turro and Khudyakov studies [36]. LFP experiments support the EPR results with the formation of (**1**) at 400 nm (see Figure S11 in Supporting Information). The transient of the diphenylphosphinoyl radical at ~ 325 nm is not observed because of the overlap of the ground state absorption/ground state bleaching of PM.

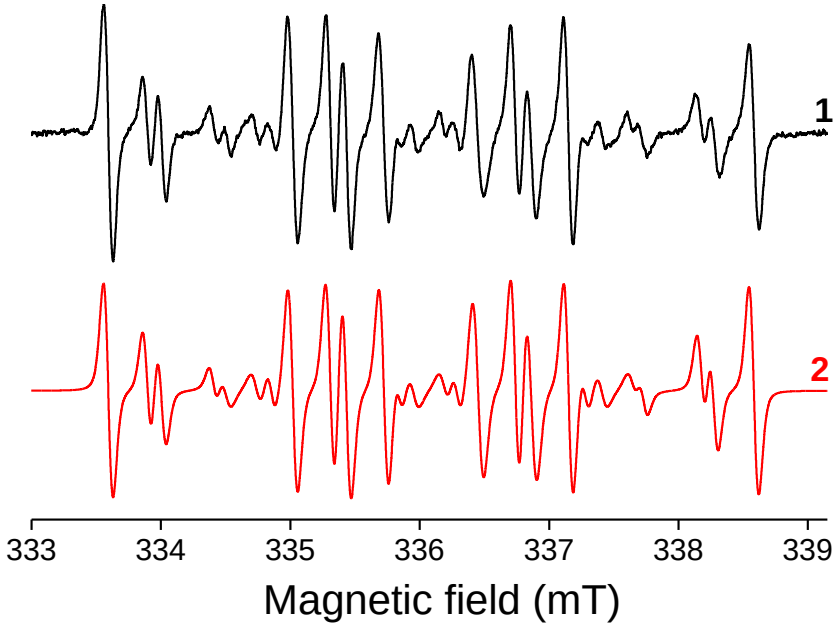

Figure 1. Experimental (1) and simulated (2) EPR spectra obtained after 900-s LED@385 nm exposure of PM/benzene solution in the presence of PBN spin trap under argon. EPR spectrometer settings: microwave frequency, ~ 9.436 GHz; microwave power, 1.114 mW; center field, 336.0 mT; sweep width, 7 mT; gain, 1.00×10^5; modulation amplitude, 0.01 mT; scan, 90 s; time constant, 20.48 ms; number of scans, 10.

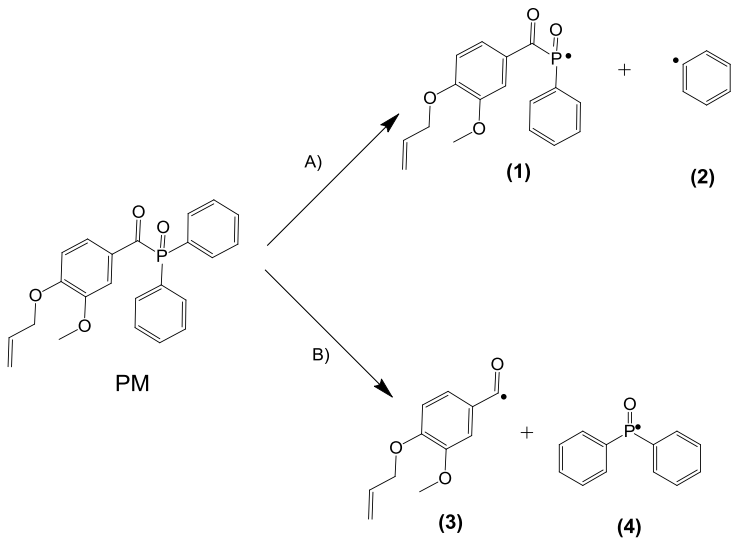

Scheme 2. Homolytic cleavage of PM under light exposure according to two photochemically pathways (A and B).

Irradiation of a benzene solution of the PM/TT photoinitiating system in the presence of DMPO using LED@385 nm leads to an immediate formation of dominant signal characterized by the spin-Hamiltonian parameters fully compatible with the •DMPO-SR spin-adduct [27] (a_N = 1.347 mT, a_H^β = 1.178 mT, a_H = 0.091 mT, a_H = 0.094 mT; g = 2.0061). This statement confirms the formation of thiyl radicals and the capability of radicals (**1**-**4** in Scheme 2) to abstract H-atom from the thiol group of TT under light exposure. Simultaneously, upon *in situ* irradiation the generation of further signals corresponding to the DMPO-adducts of phosphorus- and carbon-centered radicals is detectable, along with the low-intensity nine-line signal well compatible with the addition of hydrogen radical to DMPO (a_N = 1.455 mT, a_H^β = 1.907 mT, a_H^β = 1.898 mT; g = 2.0059). As the stability of these DMPO-adducts is low under given experimental conditions, they disappeared from spectrum after switch-off the light source and •DMPO-SR signal dominates the EPR spectrum (Figure 2). Interestingly, the quenching rate constant of PM by TT and labelled k_q^{TT} (PM) was evaluated at 0.67 × 10^8 $M^{-1}s^{-1}$ (see Figure S12 in Supporting Information for details). The high reactivity of (**1**)-(**4**) (Scheme 2) toward H-donor molecules is a consequence of the high degree of s-character and spin density localized on the carbonyl carbon, phenyl carbon and phosphorus atoms [30].

Table 2. Spin-Hamiltonian parameters of •PBN-adducts elucidated from the simulation analysis of experimental EPR spectrum shown in Figure 1.

Hyperfine coupling constants (mT)			*g*-value	Rel. concentration (%)	Radical trapped	References
a_N	a_H	a_P				
1.426	0.305	1.841	2.0060	41.8	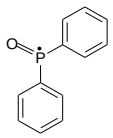	[37, 38]
1.441	0.412	1.714	2.0060	38.6	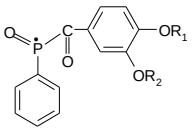	[39]
1.442	0.452	–	2.0061	7.5	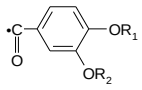	[37, 38]
1.459	0.240	–	2.0061	12.1		[27, 28]

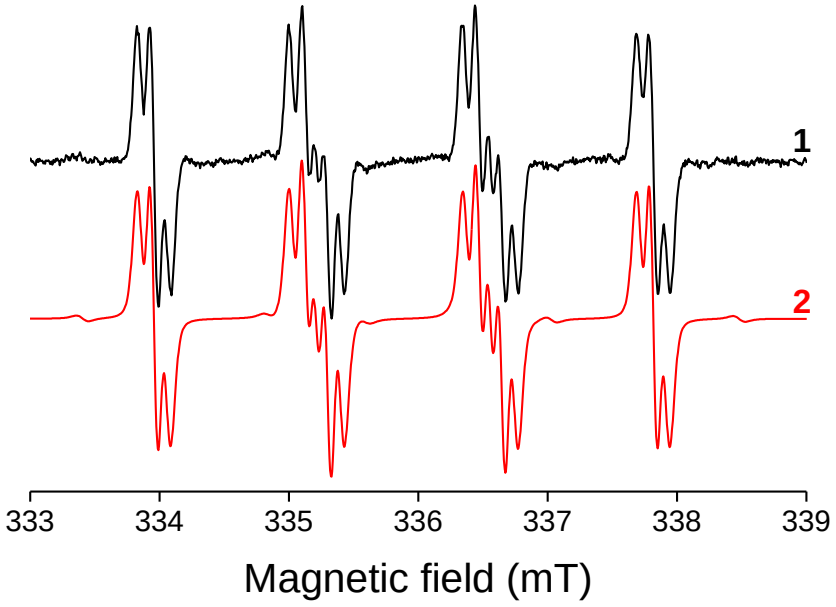

Figure 2. Experimental (1) and simulated (2) EPR spectra obtained in PM/Trithiol/benzene solution with DMPO spin trap under argon after 600-s LED@385 nm exposure. EPR spectrometer parameters: microwave frequency, ~ 9.431 GHz; microwave power, 1.087 mW; center field, 336.0 mT; sweep width, 10 mT; gain, 1.00×10^5; modulation amplitude, 0.025 mT; scan, 60 s; time constant, 20.48 ms; number of scans, 10.

To confirm the reactivity of PM toward acrylate monomers and its capability to initiate FRP under light irradiation, RT-FTIR experiments have been performed with TMPTA (Figure 3) and a bio-sourced acrylate monomer SOA (Figure 4). TMPTA was used as a reference. The final acrylate conversions for TMPTA and SOA according to PM/additives photoinitiating systems are summarized in Table 3. DMPA, BAPO, HCPK, QUIN/TT, PUR/TT AQ/TT and TX/TT were used as references for the FRP. DMPA photolyzes to produce both dimethoxybenzyl and carbonyl radicals [40], BAPO generates both benzoyl and phosphinoyl radicals [41], and AQ, QUIN, PUR and TX were used as type II photoinitiators when coupled with TT. TMPTA (Figure 3) or SOA (Figure 4) successfully polymerized in laminate when PM is used alone as a free-radical photoinitiator under light irradiation. Indeed, phosphinoyl and phenyl radicals are well-known to be reactive toward acrylate functions [27, 41]. Not surprisingly, no polymerization occurs under air with TMPTA: the dissolved oxygen gets consumed by addition to initiator radicals and radicals of the growing polymer chain to form peroxyl radicals which are unreactive toward acrylate monomers [42]. As an example, PM is quenched by molecular oxygen efficiently with a quenching rate constant k_q^{O2} (PM) which is evaluated to be 10^9 $M^{-1}s^{-1}$ (see Figure S13 in supporting information). On the opposite, PM promotes the FRP of SOA (Figure 4) under air with relatively high final conversion (40%) compared to that of TMPTA (0%): indeed, the high viscosity of SOA (1200 cps) compared to TMPTA (70-120 cps) reduces the diffusion of oxygen from the outside to the polymer coating, speeding up the FRP of SOA. Other features can be expressed when PM is coupled with TT. As expected, the FRP of SOA successfully occurs in laminate or under air with PM/TT systems; indeed, previous investigations [10, 11, 26, 27] supported the fact that thiyl radicals play a dual role i.e. they consumed dissolved oxygen, and the resulting peroxyl radicals can abstract hydrogen from TT to re-initiate the FRP (r1-r4). It is also noticeable that PM is more efficient than DMPA to initiate the FRP of TMPTA. This difference may be explained by the fact that the photolysis of PM leads to highly reactive phenyl radicals altogether with phosphinoyl and carbonyl radicals, unlike DMPA which generates only dimethoxybenzyl and carbonyl radicals [43]. Finally, PM also shows initiating properties as effective as those of the well-known type I photoinitiator BAPO (Figure 5): indeed, BAPO like PM produces benzoyl and phosphinoyl radical species after its photolysis [41].

$$PM + RSH + h\nu \rightarrow \text{phosphinoyl/carbon centered radicals} + RS^{\bullet} \quad (r1)$$

$$RS^{\bullet} + O_2 \rightarrow RSOO^{\bullet} \quad (r2)$$

$$RSOO^{\bullet} + RSH \rightarrow RSOOH + RS^{\bullet} \quad (r3)$$

$RS^{\bullet}$ + acrylate → poly(acrylate) (r4)

Table 3. Final acrylate conversions of TMPTA and SOA determined by IR with different photoinitiating systems after 800 s of irradiation.

Photoinitiating systems	TMPTA and SOA	
	Under air	In laminate
PM	np[a] (40%)[b]	72% [a] (86%)[b]
BAPO	-	70% [a] (92%)[b]
DMPA	np[a]	60%[a]
HCPK	np[a]	70%[a]
AQ/TT (1 wt%)	16%[a] (70%)[b]	71%[a] (87%)[b]
QUI/TT (1 wt%)	np[a] (np)[b]	42%[a] (31%)[b]
PUR/TT (1 wt%)	np[a] (15%)[b]	65%[a] (51%)[b]
TX / TT (1 wt%)	np[a]	55%[a]
PM / TT (1 wt%)	np[a] (50%)[b]	72%[a] (90%)[b]
PM / TT (3 wt%)	25%[a] (60%)[b]	70%[a] (90%)[b]

a = photopolymerization of TMPTA, b = photopolymerization of SOA, np = no polymerization.

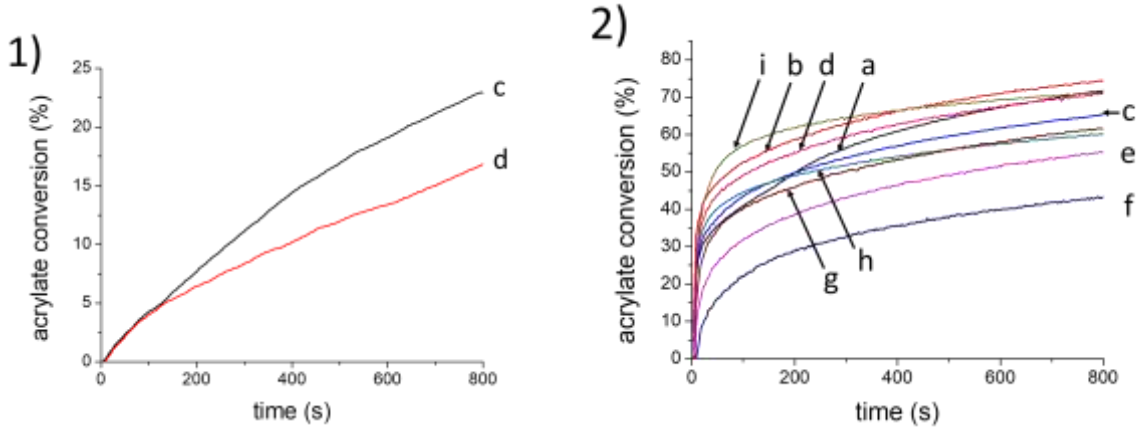

Figure 3. Kinetic profiles of the free-radical photopolymerization of TMPTA 1) under air and 2) in laminate in the presence of (a) PM (1wt%), (b) PM/TT (1/1 wt%), (c) PM/TT (1/3 wt%), (d) AQ/TT (1/1 wt%), (e) TX/TT (1/1 wt%), (f) QUI/TT (1/1 wt%), (g) PUR/TT (1/1 wt%), (h) DMPA (1 wt%) and (i) HCPK (1 wt%) upon Hg-Xe lamp irradiation (60 mW/cm^2).

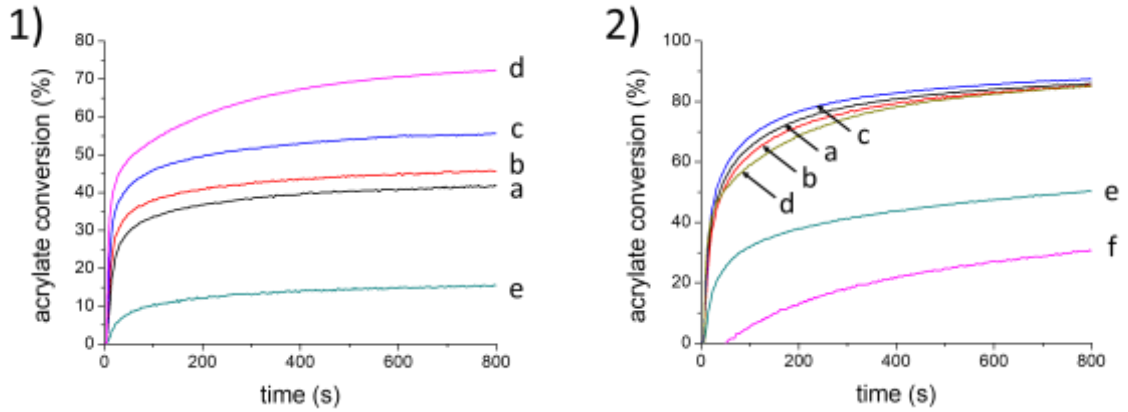

Figure 4. Kinetic profiles for the free-radical photopolymerization of SOA 1) under air and 2) in laminate in the presence of (a) PM (1 wt%), (b) PM/TT (1/1 wt%), (c) PM/TT (1/3 wt%), (d) AQ/TT (1/1 wt%), (e) PUR/TT (1/1 wt%) and (f) QUI/TT (1/1 wt%) upon Hg-Xe lamp irradiation (60 mW/cm^2).

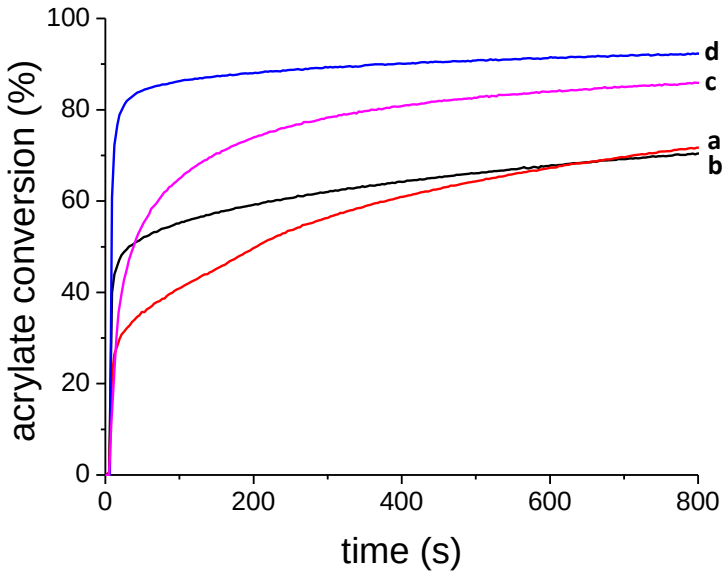

Figure 5. Kinetic profiles for the free-radical photopolymerizations (FRP) of TMPTA in laminate with a) PM (1 wt%) and b) BAPO (1 wt%) and FRP of SOA in the presence of c) PM (1 wt%) and d) BAPO (1 wt%) upon Hg-Xe lamp irradiation (60 mW/cm^2).

CONCLUSIONS

This study presents the first example of vanillin derived type I photoinitiator upon light activation. The photolysis of PM has led to the formation of phenyl, carbonyl and highly reactive phosphinoyl radicals, which can initiate the FRP of both triacrylate and natural oil acrylate monomers with high final conversions even under air. PM/thiol photoinitiating systems also demonstrate their ability to promote the synthesis of a bio-based polyacrylate despite the scavenging effect of oxygen toward radicals.

Acknowledgment

We would like to thank French Research National Agency (ANR), UPEC and ICMPE for financial help. This work was supported by a grant from the Ministère de l'Education Nationale, de l'Enseignement Supérieur et de la Recherche, Université Paris-Est Créteil (UPEC), for Louise Breloy's Ph.D. thesis. This work was supported by the Slovak Research and Development Agency under the contract No. APVV-15-0053. Vlasta Brezová thanks Ministry of Education, Science, Research and Sport of the Slovak Republic for funding within the scheme "Excellent research teams".

REFERENCES

[1] C. Mendes-Felipe, J. Oliveira, I. Etxebarria, J.L. Vilas-Vilela, S. Lanceros-Mendez, State-of-the-Art and Future Challenges of UV Curable Polymer-Based Smart Materials for Printing Technologies, Adv. Mater. Technol. 4(3) (2019) 1800618.DOI: 10.1002/admt.201800618

[2] Y. Yagci, S. Jockusch, N.J. Turro, Photoinitiated Polymerization: Advances, Challenges, and Opportunities, Macromolecules 43(15) (2010) 6245-6260. DOI: 10.1021/ma1007545

[3] S. Chatani, C.J. Kloxin, C.N. Bowman, The power of light in polymer science: photochemical processes to manipulate polymer formation, structure, and properties, Polym. Chem. 5(7) (2014) 2187-2201. DOI: 10.1039/C3PY01334K

[4] H.F. Gruber, Photoinitiators for free radical polymerization, Progr. Polym. Sci. 17(6) (1992) 953-1044. DOI: 10.1016/0079-6700(92)90006-K

[5] J.-P. Fouassier, J. Lalevée, Photoinitiators for polymer synthesis : scope, reactivity and efficiency, Wiley-VCH, Weinheim, Germany, 2012.

[6] K. Dietliker, A Compilation of Photoinitiators Commercially Available for UV Today, SITA Technology Ltd.:, London, UK, 2002.

[7] T. Sumiyoshi, W. Schnabel, On the reactivity of phosphonyl radicals towards olefinic compounds, Makromol. Chem. 186(9) (1985) 1811-1823. DOI: 10.1002/macp.1985.021860910

[8] T. Sumiyoshi, W. Schnabel, A. Henne, The photolysis of acylphosphine oxides: III: Laser flash photolysis studies with pivaloyl compounds, J. Photochem. 32(2) (1986) 191-201.DOI: 10.1016/0047-2670(86)87008-3

[9] K. Dietliker, Chemistry and Technology of UV and EB Formulation for Coatings, Inks & Paints, SITA Technology1991.

[10] C.E. Hoyle, T.Y. Lee, T. Roper, Thiol–enes: Chemistry of the past with promise for the future, J. Polym. Sci. Part A: Polym. Chem. 42(21) (2004) 5301-5338. DOI: 10.1002/pola.20366.

[11] C.E. Hoyle, A.B. Lowe, C.N. Bowman, Thiol-click chemistry: a multifaceted toolbox for small molecule and polymer synthesis, Chem. Soc. Rev. 39(4) (2010) 1355-1387. DOI: 10.1039/B901979K.

[12] N.B. Cramer, C.N. Bowman, Kinetics of thiol–ene and thiol–acrylate photopolymerizations with real-time fourier transform infrared, J. Polym. Sci. Part A: Polym. Chem. 39(19) (2001) 3311-3319. DOI: 10.1002/pola.1314

[13] M. El-Roz, J. Lalevée, X. Allonas, J.P. Fouassier, Mechanistic Investigation of the Silane, Germane, and Stannane Behavior When Incorporated in Type I and Type II Photoinitiators of Polymerization in Aerated Media, Macromolecules 42(22) (2009) 8725-8732. DOI: 10.1021/ma9017313

[14] P. Gauss, M. Griesser, M. Markovic, A. Ovsianikov, G. Gescheidt, P. Knaack, R. Liska, α-Ketoesters as Nonaromatic Photoinitiators for Radical Polymerization of (Meth)acrylates, Macromolecules 52(7) (2019) 2814-2821.DOI: 10.1021/acs.macromol.8b02640.

[15] A. Ledwith, M.D. Purbrick, Initiation of free-radical polymerization by photoinduced electron transfer processes, Polymer 14(10) (1973) 521-522. DOI: 10.1016/0032-3861(73)90162-6

[16] R.S. Davidson, The Chemistry of Excited Complexes: a Survey of Reactions, in: V. Gold, D. Bethell (Eds.), Advances in Physical Organic Chemistry, Academic Press1983, pp. 1-130.

[17] J. Hutchison, M.C. Lambert, A. Ledwith, Rôle of semi-pinacol radicals in the benzophenone-photoinitiated polymerization of methyl methacrylate, Polymer 14(6) (1973) 250-254. DOI: 10.1016/0032-3861(73)90084-0

[18] M. Fache, B. Boutevin, S. Caillol, Vanillin Production from Lignin and Its Use as a Renewable Chemical, ACS Sustain. Chem. Eng. 4(1) (2016) 35-46. DOI: 10.1021/acssuschemeng.5b01344.

[19] D.J. Fitzgerald, M. Stratford, M.J. Gasson, J. Ueckert, A. Bos, A. Narbad, Mode of antimicrobial action of vanillin against Escherichia coli, Lactobacillus plantarum and Listeria innocua, J. Appl. Microbiol. 97(1) (2004) 104-113. DOI:10.1111/j.1365-2672.2004.02275.x
[20] S. Kamaraj, U.M. Palanisamy, M.S.B. Kadhar Mohamed, A. Gangasalam, G.A. Maria, R. Kandasamy, Curcumin drug delivery by vanillin-chitosan coated with calcium ferrite hybrid nanoparticles as carrier, Eur. J. Pharm. Sci. 116 (2018) 48-60. DOI:10.1016/j.ejps.2018.01.023.
[21] P. Zhao, Z. Liu, X. Wang, Y.-T. Pan, I. Kuehnert, M. Gehde, D.-Y. Wang, A. Leuteritz, Renewable vanillin based flame retardant for poly(lactic acid): a way to enhance flame retardancy and toughness simultaneously, RSC Adv. 8(73) (2018) 42189-42199. DOI: 10.1039/c8ra08531e
[22] X. Xu, S. Wang, S. Ma, W. Yuan, Q. Li, J. Feng, J. Zhu, Vanillin-derived phosphorus-containing compounds and ammonium polyphosphate as green fire-resistant systems for epoxy resins with balanced properties, Polym. Adv. Technol. 30(2) (2019) 264-278. DOI: 10.1002/pat.4461
[23] M. Stroescu, A. Stoica-Guzun, G. Isopencu, S.I. Jinga, O. Parvulescu, T. Dobre, M. Vasilescu, Chitosan-vanillin composites with antimicrobial properties, Food Hydrocoll. 48 (2015) 62-71. DOI: 10.1016/j.foodhyd.2015.02.008
[24] M. Fache, E. Darroman, V. Besse, R. Auvergne, S. Caillol, B. Boutevin, Vanillin, a promising biobased building-block for monomer synthesis, Green Chem. 16(4) (2014) 1987-1998. DOI: 10.1039/C3GC42613K
[25] M. Fache, B. Boutevin, S. Caillol, Vanillin, a key-intermediate of biobased polymers, Eur. Polym. J. 68 (2015) 488-502. DOI: 10.1016/j.eurpolymj.2015.03.050
[26] L. Breloy, C.A. Ouarabi, A. Brosseau, P. Dubot, V. Brezova, S. Abbad Andaloussi, J.-P. Malval, D.-L. Versace, β-Carotene/Limonene Derivatives/Eugenol: Green Synthesis of Antibacterial Coatings under Visible-Light Exposure, ACS Sustain. Chem. Eng. 7(24) (2019) 19591-19604. DOI: 10.1021/acssuschemeng.9b04686
[27] L. Breloy, V. Brezová, J.-P. Malval, A. Rios de Anda, J. Bourgon, T. Kurogi, D.J. Mindiola, D.-L. Versace, Well-Defined Titanium Complex for Free-Radical and Cationic Photopolymerizations under Visible Light and Photoinduction of Ti-Based Nanoparticles, Macromolecules 52(10) (2019) 3716-3729. DOI: 10.1021/acs.macromol.8b02719
[28] L. Breloy, V. Brezová, A. Blacha-Grzechnik, M. Presset, M.S. Yildirim, I. Yilmaz, Y. Yagci, D.-L. Versace, Visible Light Anthraquinone Functional Phthalocyanine Photoinitiator for Free-Radical and Cationic Polymerizations, Macromolecules 53(1) (2020) 112-124. DOI: 10.1021/acs.macromol.9b01630
[29] R. Nazir, P. Danilevicius, D. Gray, M. Farsari, D.T. Gryko, Push–Pull Acylo-Phosphine Oxides for Two-Photon-Induced Polymerization, Macromolecules 46(18) (2013) 7239-7244. DOI: 10.1021/ma4010988
[30] G.W. Sluggett, C. Turro, M.W. George, I.V. Koptyug, N.J. Turro, (2,4,6-Trimethylbenzoyl)diphenylphosphine Oxide Photochemistry. A Direct Time-Resolved Spectroscopic Study of Both Radical Fragments, J. Am. Chem. Soc. 117(18) (1995) 5148-5153. DOI: 10.1021/ja00123a018
[31] C. Dursun, M. Degirmenci, Y. Yagci, S. Jockusch, N.J. Turro, Free radical promoted cationic polymerization by using bisacylphosphine oxide photoinitiators: substituent effect on the reactivity of phosphinoyl radicals, Polymer 44(24) (2003) 7389-7396. DOI: 10.1016/j.polymer.2003.09.020
[32] T. Sumiyoshi, W. Schnabel, A. Henne, P. Lechtken, On the photolysis of acylphosphine oxides: 1. Laser flash photolysis studies with 2,4,6-trimethylbenzoyldiphenylphosphine oxide, Polymer 26(1) (1985) 141-146. DOI: 10.1016/0032-3861(85)90069-2

[33] H. M. Swartz, N. Khan, V.V. Khramtsov, Use of Electron Paramagnetic Resonance Spectroscopy to Evaluate the Redox State In Vivo, Antioxid. Redox Signal. 9(10) (2007) 1757-1772. DOI: 10.1089/ars.2007.1718
[34] W.G. Hatton, N.P. Hacker, P.H. Kasai, The photochemistry of nitrosobenzene: direct observation of the phenyl radical–nitric oxide triplet radical pair in argon at 12 K, J. Chem. Soc., Chem. Comm. (3) (1990) 227-229. DOI: 10.1039/C39900000227
[35] J. Bartl, S. Steenken, H. Mayr, R.A. McClelland, Photo-heterolysis and -homolysis of substituted diphenylmethyl halides, acetates, and phenyl ethers in acetonitrile: characterization of diphenylmethyl cations and radicals generated by 248-nm laser flash photolysis, J. Am. Chem. Soc. 112(19) (1990) 6918-6928. DOI: 10.1021/ja00175a028
[36] N.J. Turro, I.V. Khudyakov, Single-phase primary electron spin polarization transfer in spin-trapping reactions, Chem. Phys. Lett. 193(6) (1992) 546-552. DOI: 10.1016/0009-2614(92)85846-3
[37] F. Morlet-Savary, J.E. Klee, F. Pfefferkorn, J.P. Fouassier, J. Lalevée, The Camphorquinone/Amine and Camphorquinone/Amine/Phosphine Oxide Derivative Photoinitiating Systems: Overview, Mechanistic Approach, and Role of the Excitation Light Source, Macromol. Chem. Phys. 216(22) (2015) 2161-2170. DOI: 10.1002/macp.201500184
[38] A. Criqui, J. Lalevée, X. Allonas, J.-P. Fouassier, Electron Spin Resonance Spin Trapping Technique: Application to the Cleavage Process of Photoinitiators, Macromol. Chem. Phys. 209(21) (2008) 2223-2231. DOI: 10.1002/macp.200800303
[39] S. Yoshimi, M. Yuzo, Spin Trapping of Phosphorus-Centered Radicals Produced by the Reactions of Dibenzoyl Peroxide with Organophosphorus Compounds, Bull. Chem. Soc. Jap. 70(2) (1997) 397-403. DOI: 10.1246/bcsj.70.397
[40] D.-L. Versace, J.-P. Fouassier, J. Lalevée, The First Photochemical In Situ Production of Ti-Based Nanoparticles: A SH2 Strategy Using Bis(cyclopentadienyl)titanium Dichloride (Cp2TiCl2), Macromol. Rapid Comm. 35(8) (2014) 821-826. DOI: 10.1002/marc.201300924
[41] R. Copperwhite, M. Oubaha, D.L. Versace, C. Croutxé-Barghorn, B.D. MacCraith, The role of photoinitiator and chelating agent in the fabrication of optical waveguides from UV-photocurable organo-mineral sol–gel materials, J. Non-Cryst. Solids 354(30) (2008) 3617-3622. DOI: 10.1016/j.jnoncrysol.2008.03.026
[42] A.K. O'Brien, C.N. Bowman, Impact of Oxygen on Photopolymerization Kinetics and Polymer Structure, Macromolecules 39(7) (2006) 2501-2506. DOI: 10.1021/ma051863l
[43] D.L. Versace, J. Bourgon, E. Leroy, F. Dumur, D. Gigmes, J.P. Fouassier, J. Lalevée, Zinc complex based photoinitiating systems for acrylate polymerization under air; in situ formation of Zn-based fillers and composites, Polym. Chem. 5(22) (2014) 6569-6576. DOI: 10.1039/C4PY00716F